Cell, Vol. 102, 671–682, September 1, 2000, Copyright ©2000 by Cell Press

# A Novel Genetic Pathway for Sudden Cardiac Death via Defects in the Transition between Ventricular and Conduction System Cell Lineages

**Vân T. B. Nguyên-Trân,[1] Steven W. Kubalak,[3] Susumu Minamisawa,[1,10] Céline Fiset,[4,6] Kai C. Wollert,[1,8] Anne B. Brown,[1,9] Pilar Ruiz-Lozano,[1] Stéphanie Barrere-Lemaire,[1,7] Richard Kondo,[1] Lisa W. Norman,[3] Robert G. Gourdie,[3] Marc M. Rahme,[2] Gregory K. Feld,[2] Robert B. Clark,[4] Wayne R. Giles,[4] and Kenneth R. Chien[1,5]**

[1] UCSD-Salk Program in Molecular Medicine and the UCSD Institute of Molecular Medicine

[2] Department of Medicine
University of California, San Diego
La Jolla, California 92093

[3] Department of Cell Biology and Anatomy
Medical University of South Carolina
Charleston, South Carolina 29425

[4] University of Calgary
Calgary T2N 4N1
Canada

## Summary

**HF-1b, an SP1-related transcription factor, is preferentially expressed in the cardiac conduction system and ventricular myocytes in the heart. Mice deficient for HF-1b survive to term and exhibit normal cardiac structure and function but display sudden cardiac death and a complete penetrance of conduction system defects, including spontaneous ventricular tachycardia and a high incidence of AV block. Continuous electrocardiographic recordings clearly documented cardiac arrhythmogenesis as the cause of death. Single-cell analysis revealed an anatomic substrate for arrhythmogenesis, including a decrease and mislocalization of connexins and a marked increase in action potential heterogeneity. Two independent markers reveal defects in the formation of ventricular Purkinje fibers. These studies identify a novel genetic pathway for sudden cardiac death via defects in the transition between ventricular and conduction system cell lineages.**

## Introduction

Sudden cardiac death is a leading cause of cardiovascular mortality, accounting for the loss of ~400,000 lives in the United States each year (Zipes and Wellens, 1998). In most cases, the underlying cause of death is the rapid onset of lethal ventricular arrhythmias in the setting of acquired heart disease. The onset of sudden cardiac death is multifactorial, and the elucidation of the precise molecular and cellular pathways responsible for this phenotype has been difficult due to the paucity of genetic insights into this complex human cardiac disease. The discovery of mutations in specific cardiac voltage-gated $K^+$ channels in patients with long QT syndrome and their role in slowing cardiac repolarization has provided a potential mechanistic link with some of these acquired arrhythmias (for a review see Curran et al., 1999). However, studies of affected families have revealed that only 20% of the patients who harbor the disease genotype display sudden death (Roden and Spooner, 1999), suggesting the requirement of additional pathways that must be present to produce the disease phenotype. Further evidence of the requirement of a "second hit" to produce lethal ventricular arrhythmogenesis has come from studies of genetically engineered mice that harbor mutations in the cardiac $Na^+$ or $K^+$ channels that produce long QT syndrome, prolonged cardiac repolarization, and associated arrhythmias, but not sudden cardiac death (Barry et al., 1998; Charpentier et al., 1998; Drici et al., 1998; London et al., 1998; Abbott et al., 1999; Kupershmidt et al., 1999). Currently, there are no accepted clinical criteria to unequivocally identify high-risk patients, and existing therapy for survivors of sudden cardiac death is palliative, primarily based upon implantable defibrillators. The development of biologically targeted therapy for this disease will first require the identification of new mechanistic pathways that can lead to sudden cardiac death in experimental systems. Presently, there are few reliable experimental systems in which spontaneous cardiac sudden death can be studied. While the mouse has been valuable as a tool to reveal new signaling pathways that drive complex features of dilated cardiomyopathy and heart failure (Coral-Vazquez et al., 1999; Chien, 1999; Hirota et al., 1999; Minamisawa et al., 1999), there have been no previous reports of genetically engineered mouse models of primary sudden cardiac death.

The establishment of organized, rapid cardiac conduction is dependent on the recruitment of cardiomyocytes into conduction system lineages (Gourdie et al., 1999). Synchronous generation of action potentials in distinct conduction system cell lineages is essential for orderly impulse propagation. A critical feature of ventricular arrhythmogenesis in cardiomyopathy and associated heart failure is the heterogeneity of action potential duration (APD), a significant clinical risk factor for cardiac sudden death (for a review see Marban, 1999). The mechanistic basis for this action potential heterogeneity is not understood, but conceptually, defects in the recruitment of conduction system cell lineages might be a contributing factor. In this manner, genes that guide and/or maintain the electrophysiological transition between ventricular and conduction cell lineages might play a critical primary role in the onset of lethal arrhythmias and sudden cardiac death, even in the absence of

[5] To whom correspondence should be addressed (e-mail: kchien@ucsd.edu).

[6] Present address: Montreal Heart Institute, Montreal, Quebec H1T 1C8, Canada.

[7] Present address: Institut de Genetique Humaine-CNRS UPR 1142, 34396 Montpellier Cedex 5, France.

[8] Present address: Department of Cardiology and Angiology, Medizinische Hochschule Hannover, Carl-Neuberg Str. 1, 30625 Hannover, Germany.

[9] Present address: AGI Dermatics, Freeport, New York 11520.

[10] Present address: The Heart Institute of Japan, Tokyo Women's Medical University, Shinjuku-ku, Tokyo 162-8666, Japan.

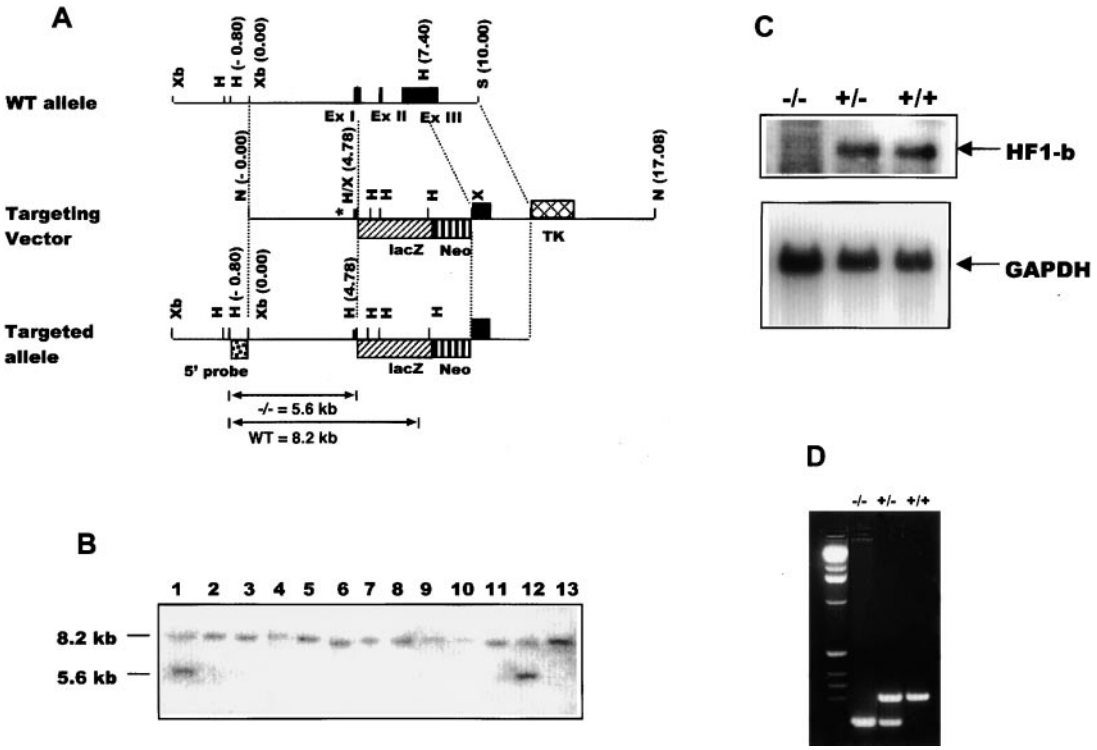


Figure 1. Gene Targeting Strategy of *HF-1b* Locus

(A) Diagram of the *HF-1b* endogenous locus, the targeting construct, and the resulting targeted *HF-1b* locus. Exons are denoted as solid black rectangles. Restriction sites are as follows: X = XhoI, H = HpaI, Xb = XbaI, N = NotI, and S = SalI.

(B) Representative Southern blot of genomic DNA from 13 ES clones; clones 1 and 12 show the mutant allele as a result of homologous recombination.

(C) Northern blot analysis of RNAs from wild-type (+/+), heterozygous (+/−), and homozygous (−/−) *HF-1b* mice.

(D) Detection of wild-type (+/+) and mutant alleles by PCR analysis of genomic DNA from tail biopsies of progeny from a heterozygous × heterozygous cross. The genotypes and their corresponding PCR products are as follows: *HF-1b*$^{-/-}$ = 250 bp; *HF-1b*$^{+/-}$ = 354 bp and 250 bp; *HF-1b*$^{+/+}$ = 354 bp.

overt heart failure or hypertrophy. Via the generation of mice that harbor a deficiency in a cardiac transcription factor that is enriched in ventricular and conduction system lineages, the present study provides direct evidence for this novel pathway for sudden cardiac death.

## Results

### Generation of *HF-1b* Null Allele Mice

*HF-1b* is a cardiac transcription factor related to the SP-1 gene family (Zhu et al., 1993). An earlier gene targeting study of *HF-1b* (or *Sp4*), where only the DNA binding domains were removed, revealed that *HF-1b*/*Sp4* is essential for normal murine growth (Supp et al., 1996). Since this gene targeting strategy could potentially result in a hypomorphic and/or dominant-negative allele versus a true null allele, we introduced a *lacZ* reporter gene into the endogenous locus of *HF-1b* that eliminated the start codon (Figure 1A). Two targeted embryonic stem cell clones were used to establish mouse lines carrying the *HF-1b* mutation (Figure 1B), resulting in the complete inactivation of the endogenous gene as assessed by Northern blot analyses (Figure 1C) and also allowing phenotypic characterization of offspring from heterozygous intercrosses (Figure 1D). *HF-1b*$^{-/-}$ mice appeared with the expected Mendelian frequency, thereby indicating no embryonic lethality. Unlike the previously reported Sp4 knockout mice, which have a high perinatal mortality rate (i.e., two-thirds die within the first few days after birth), ~40% of the *HF-1b* mice survive beyond 6–8 months. The surviving *HF-1b*-deficient animals are relatively smaller in size compared to their control littermates and are reproductively sterile.

### Preferential Expression of *HF-1b* in Ventricular and Cardiac Conduction System Cell Lineages in the Developing Heart

During early embryogenesis, *HF-1b* is expressed predominantly in the developing neuroepithelium and the central nervous system with a uniformly low level of expression in the ventricular segment of the developing heart tube at E8.5 postcoitum (pc) (data not shown). By day 12.5 pc, *HF-1b* cardiac expression is restricted to the conotruncus, specifically at the lateral limits of the conoventricular boundary and in the interventricular septum with little or no detectable expression in the atrial chamber (Figure 2A). This predominantly ventricular restricted pattern is maintained from E13.5 pc (Figure 2B) up to E17.5 pc, when a gradient is established that reveals a higher level of *HF-1b* expression in the left

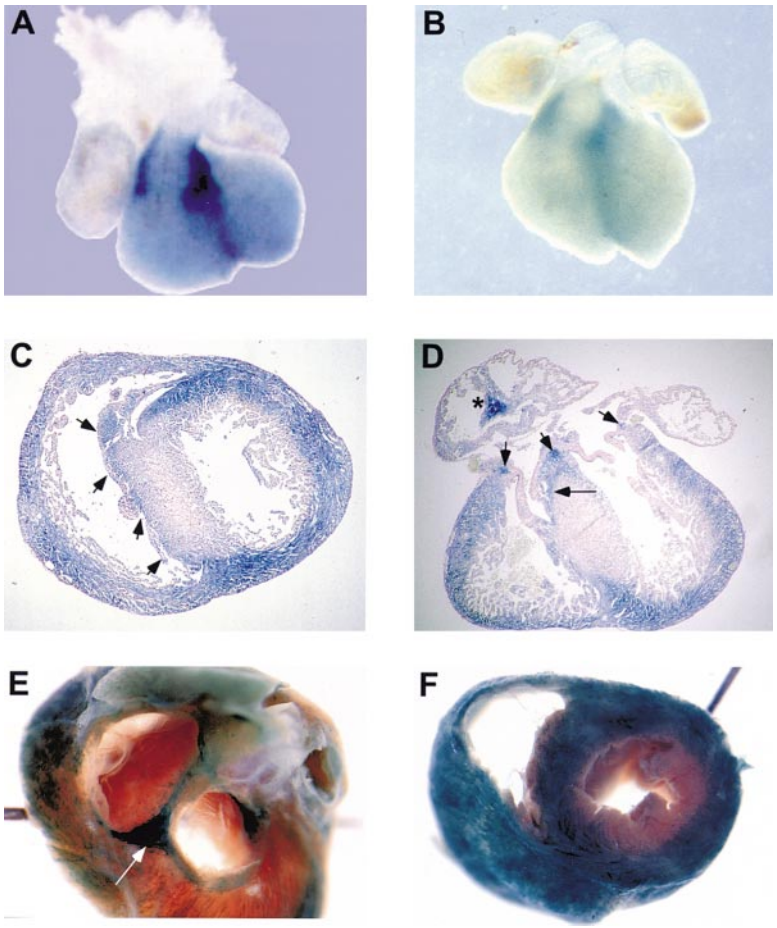


Figure 2. Developmental Pattern of *HF-1b* Expression in Embryonic Mouse Heart as Determined by *lacZ* Staining

(A) Heart from day 12.5 pc *HF-1b* embryo. (B) Hearts from day 13.5 pc wild-type, heterozygous, and homozygous *HF-1b* embryos. Transverse (C) and sagittal (D) sections from two different day 17.5 pc *HF-1b*$^{-/-}$ embryos. (E and F) Serial transverse sections from an adult *HF-1b*$^{+/-}$ mouse. *lacZ* staining in putative Purkinje cells (C, arrows), and in AV ring, His bundle, and bundle branches of the central conduction system (D, arrows). Asterisk in (D) indicates localized *lacZ* staining in the right atrial appendage.

versus the right ventricle (Figures 2C and 2D). The highest level of *lacZ* staining coincides with the developing conduction system. *lacZ*-positive cells were observed on the most anterior aspect of the interventricular septum and in a subpopulation of subendocardial cells extending down either side of the septum, particularly on the right ventricular side reminiscent of the branching bundles and Purkinje fibers of the ventricular conduction system (Figures 2C and 2D, arrows). *lacZ*-positive cells were also localized to a very discrete region in the right atrium (Figure 2D, asterisk). In the adult heart, the clusters of supravalvular cardiomyocytes with the most intensely blue *lacZ* staining coincided with the primary atrioventricular ring (Figure 2E, arrowhead) and were in greater abundance at the apex (Figure 2F) when compared to the base (Figure 2E) of the heart. Thus, *HF-1b* appears to be preferentially expressed in the ventricular muscle and in components of the cardiac conduction system.

### *HF-1b*-Deficient Mice Display a Sudden Death Phenotype

Even though the *HF-1b* deficiency did not result in embryonic lethality, the *HF-1b*-deficient animals displayed an increased incidence of postnatal mortality (by 6–8 months of age, 59%, or 20 out of 34 *HF-1b*$^{-/-}$ mice died versus 0% for both heterozygous and wild type, i.e., 0/67 and 0/40 for $+/-$ and $+/+$, respectively, in data compiled from 16 independent litters). The manner in which these homozygous mutants died was characterized as "sudden death," since the animals were unexpectedly found dead within 24 hr of displaying relatively normal behavior and activity levels. Within one week of birth, the incidence of perinatal death for the *HF-1b*$^{-/-}$ mice amounted to 11% (or 4/34). By one month, an additional 32% (or 11/34) of *HF-1b*$^{-/-}$ mice were found dead. Of the mutant animals that survived past one month of age, 15% (or 5/34) also died unexpectedly around the age of 6–8 months despite having normal appearance and behavior the previous day.

### *HF-1b*-Deficient Mice Are Highly Susceptible to Inducible Ventricular Arrhythmias

A detailed analysis of cardiac electrophysiological function was undertaken in the surviving *HF-1b* mutant mice (Figure 3). Heart rate (HR, bpm) and PR interval (ms) were not significantly different in control ($n = 10$) and mutant ($n = 13$) mice, respectively (HR: control $= 461 \pm 51$ versus $-/- = 400 \pm 39$; PR: control $= 36 \pm 5$ versus $-/- = 38 \pm 4$). To gauge the relative inducibility of life-threatening ventricular arrhythmias, we developed an electrical stimulation protocol with a miniaturized ventricular plaque electrode designed to induce ectopic or reentrant rhythms. This approach involved performing

A

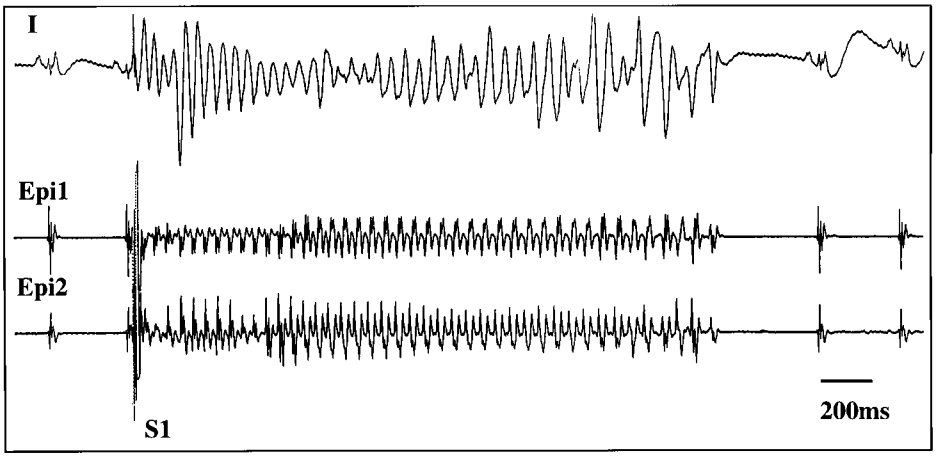


B

Summary of Electrocardiographic Data of HF-1b Mice Obtained with Implantable Radiotelemetry

| Genotype | Total Time Each Group of Mice were Monitored | Animals Found Dead | Intermittent Sinus Pauses/Sinus Blocks | AV Blocks | Spontaneous Ventricular Tachycardia | Bradycardic Arrhythmias | Premature Ventricular Contractions |
|---|---|---|---|---|---|---|---|
| (-/-) n = 11 | 166 days | 8 | 11 | 6 | 3 | 7 | 11 |
| (+/+) n = 5 | 86 days | 0 | 0 | 0 | 0 | 0 | 1 |

Figure 3. Inducible and Spontaneous Ventricular Arrhythmias in HF-*1b* Mutant Mice

(A) Representative ECG of inducible ventricular tachycardia in *HF-1b* mutant mouse. Simultaneous ECC recordings (surface lead I and two epicardial leads, Epi1 and Epi2) for a *HF-1b* mutant that experienced ventricular tachycardia resulting from programmed ventricular stimulation with a single premature stimulus ($S_1$).

(B) Summary of ECG data from *HF-1b* and wild-type mutant and mice obtained with implantable radio telemetry.

programmed ventricular stimulation during sinus rhythm and scanning diastole with a single premature stimulus ($S_1$) to determine ventricular refractoriness. Ventricular tachycardia was induced by a single extra stimulus in all of the mutant *HF-1b* mice (13 out of 13, Figure 3A). In contrast, none of the control wild-type or heterozygous animals displayed ventricular tachycardia after receiving a single extra stimulus, and only short runs of ventricular ectopic rhythm were induced following either double or triple ventricular premature stimuli. The induced arrhythmias observed in the *HF-1b*-deficient mice were primarily monomorphic (11 out of 13) but nonsustained (872 $\pm$ 683 ms VT duration; n = 12). Subsequently, a systematic examination (Kubalak et al., 1996) of the rest of the surviving *HF-1b*$^{-/-}$ mice (n = 13) for cardiac chamber volume size, wall thickness, and contractility by echocardiography and miniaturized catheterization revealed no evidence of heart failure, injury, and basal or inducible dysfunction (data not shown).

### Continuous Telemetric Monitoring Reveals Spontaneous Sudden Cardiac Death Due to Widespread Conduction Defects and Ventricular Arrhythmogenesis in *HF-1b*$^{-/-}$ Mice

To determine if life-threatening arrhythmias contributed to the sudden death of the *HF-1b* mutant mice, implantable radio telemetry was used to continuously monitor electrocardiographical data from both wild-type and mutant mice (Figure 3B). A microradio transmitter was surgically implanted to allow transmission and online recording of electrocardiogram (ECGs) from conscious, freely moving, unanesthetized mice. To capture spontaneous arrhythmias, continuous ECG recordings were acquired and stored in full waveform format. Continuous recording of 11 *HF-1b* mutant animals was acquired (total accumulated time = 166 days) to qualitatively and quantitatively evaluate the arrhythmias and to obtain unequivocal ECG evidence for authentic, spontaneous sudden death events. Littermate control mice were also examined in parallel, revealing no ECG abnormalities in over 80 days of continuous recording. The incidence of sudden death was higher in *HF-1b* mutant mice (8 out of 11) when compared to their wild-type controls (0 out of 5). The cause of death in these *HF-1b* mutant mice was clearly related to the underlying rhythm disturbances. While no arrhythmias or conduction abnormalities were observed in wild-type or heterozygous controls, there were conduction defects in the *HF-1b* mutant mice that indicated physiological dysfunction at all levels of the conduction system, i.e., SA and AV node, His bundle, and distal Purkinje fibers. All of *HF-1b* mutant mice examined had intermittent sinus pauses (Figure 4A), while none were observed in the control mice. *HF-1b* mutant mice also show a high incidence of sinus bradycardia and AV block (Figures 4B and 4C) as well as spontaneous ventricular tachycardia (Figures 4D–4E). These data are most consistent with the arrhythmias observed in the setting of end stage heart failure that can be associated with idioventricular arrhythmias as

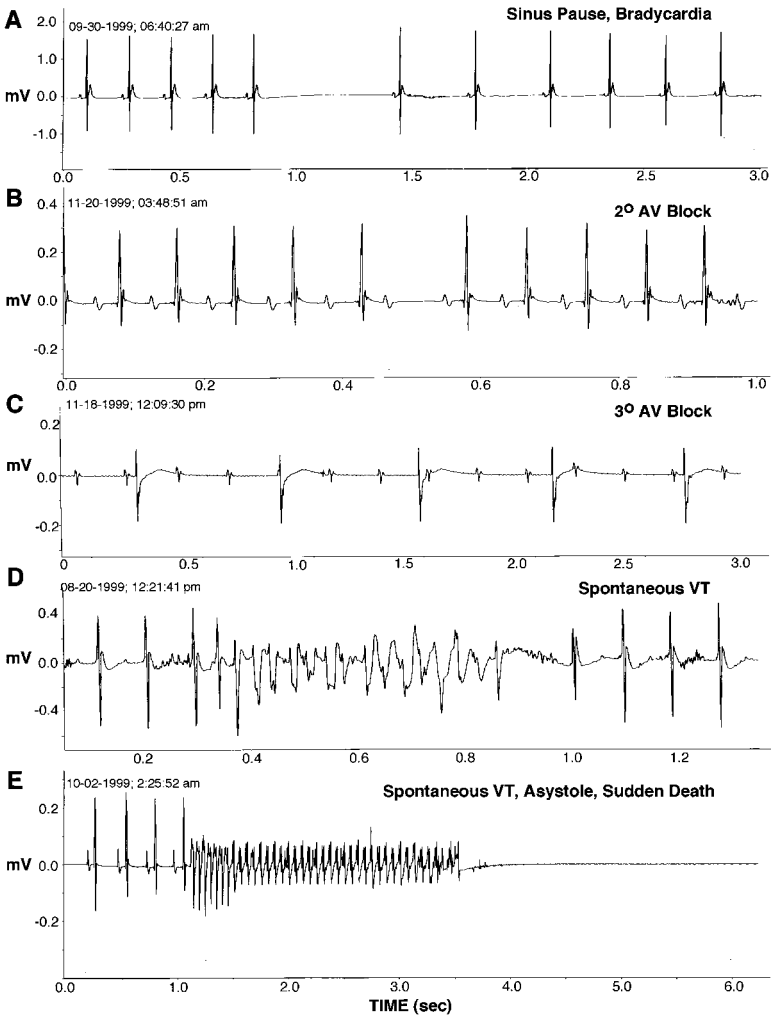


Figure 4. Representative ECGs from *HF-1b* Mutant Mice Obtained with Implantable Radio Telemetry

(A) Sinus pause and sinus bradycardia in *HF-1b* mutant mouse. AV block in *HF-1b* mutant mouse, representative example of 2° (B) and 3° AV block (C). Spontaneous ventricular tachycardia in *HF-1b* mutant mouse (D). Spontaneous ventricular tachycardia, asystole, and sudden death in an *HF-1b* mutant mouse (E).

well as ventricular arrhythmias. The pattern of arrhythmias at the time of death indicates a pattern often seen in the setting of end stage heart failure where a mixture of tachycardia and bradycardia degenerates into asystole as opposed to ventricular fibrillation (Figure 4E). However, since there was no associated evidence of hypertrophy, heart failure, or dilated cardiomyopathy, the arrhythmias in these *HF-1b* mutant animals reflects a primary electrophysiological defect as opposed to simply reflecting a secondary effect related to heart failure.

### Marked Defects in Cardiac Conduction System Cell Lineages in the HF-1b-Deficient Mice

To determine if the widespread arrhythmias reflected structural defects in the cardiac conduction system, we employed markers that differentiate the conduction tissue from ventricular myocytes. During the first 3 weeks of postnatal life, the connexins become localized in a restricted manner to the intercalated discs as the adult ventricular cells attain their rod shape and as the distal Purkinje system becomes mature (Angst et al., 1997). In the murine heart, connexin 40 (Cx40) has been shown to be a sensitive marker for central and peripheral conduction system (Gourdie et al., 1993; Delorme et al., 1995). *lacZ*-positive areas in the adult *HF-1b* mutant hearts (Figures 2E and 2F) were indeed part of the central conduction system since the same corresponding areas also costained with Cx40 and β-galactosidase (Figures 5A–5C). To establish the role of *HF-1b* in defined regions of the cardiac conduction system, we analyzed the Cx40 expression patterns in both wild-type and *HF-1b* mutant mice. Cx40 immunolocalized to the appropriate components of the conduction system, including the proximal region of the AV node, His bundle, bundle branches (data not shown), and in the peripheral Purkinje fibers in both wild-type and mutant littermates (Figures 5D–5I). However, there were distinct differences in the cellular distribution of Cx40-containing gap junctional plaques between wild-type and mutant mice, particularly in the distal Purkinje cells (Figures 5D–5I). Cx40 expression, as assessed by the number of Cx40-positive myocytes per total Purkinje cells, demonstrated there were markedly fewer cells expressing Cx40 in *HF-1b* mutant mice (45%) when compared to their littermate controls (84%) (Figure 5J). Furthermore, the distribution of Cx40 within the cells themselves was altered in *HF-1b* mutant hearts. Normally, there is a redistribution of Cx40 from the cytosol to the cell membrane during early postnatal development representing the formation of functional gap junction plaques at the cell membrane (Litchenberg et al.,

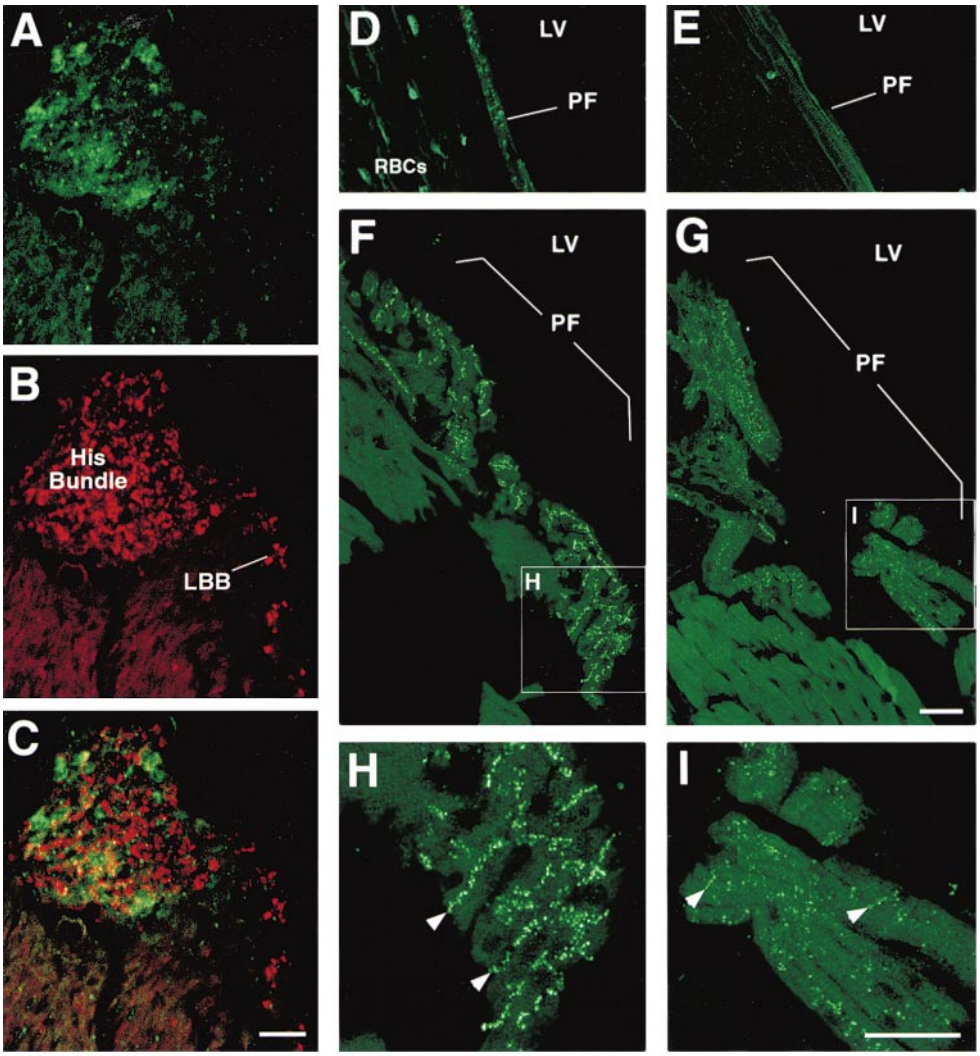


**J** **Percent Purkinje Cells Expressing Cx40**

| | WT | (-/-) |
|---|---|---|
| Number of Purkinje cells counted | 179 | 166 |
| Number of Purkinje cells Positive for Cx40 | 148 (84%) | 74 (45%) |

**K** **Distribution of Cx40 in Purkinje Cells**

| | | |
|---|---|---|
| Number of Cx40 positive Purkinje cells counted | 384 | 306 |
| Number of Purkinje cells with Cx40 aligned at cell borders | 304 (79%) | 142 (46%) |
| Number of Purkinje cells with Cx40 randomly distributed | 124 (32%) | 208 (68%) |

Figure 5. Immunolocalization of *HF-1b* and Connexin 40 in the Cardiac Conduction System

Colocalization of *HF-1b* (A) and Cx40 (B) in the AV node and branching bundle of an adult *HF-1b* mutant mouse (C). Expression pattern of connexin 40 (Cx40) in the distal Purkinje fibers of wild type (D and F) compared to *HF-1b*-deficient mouse (E and G). (H) and (I) are higher magnification views of the insets in (F) and (G). Note the more random distribution of Cx40 expression in the *HF-1b* null mutant. Alignment of Cx40 to cell borders is more easily identified in the wild-type animal (H, arrowheads) as compared to the mutant mouse (I, arrowheads). Quantitation of Cx40 expression was performed by two different criteria: (1) by determining the relative number of Cx40-positive myocytes with clusters of Purkinje cells (J) and (2) by determining the relative intracellular distribution pattern of Cx40 protein either at the cell membrane (presumably functional gap junction plaques) or randomly distributed (nonfunctional) within the cell (K). Values are representative of two separate sets of wild-type and *HF-1b* mutant hearts. All Cx40-positive areas within 2–3 separate sections were analyzed for each animal. Note that in the *HF-1b* null heart, less cells within clusters of Purkinje cells were expressing Cx40 and those that were expressing Cx40 in mutant hearts had a more random distribution pattern within the cells.

2000). In wild-type mice, ~79% of Cx40-positive Purkinje cells displayed Cx40 immunostaining distributed at the cell borders in comparison to 46% of immunopositive sites located randomly within the cell (Figures 5F, 5H, and 5K). In contrast, mutant hearts showed only 32% of Cx40-positive staining at cell borders, while 68% displayed a random distribution (Figures 5G, 5I, and 5K). These results suggest that *HF-1b*-dependent downstream pathways may play a role in trafficking of the Cx40 protein to gap junctional sites. Interestingly, we have recently detected parallel differences in the cellular distribution pattern for Cx43, a gap junction protein that is predominantly expressed in the working myocardium (L. W. N., R. S., V. T. B. N.-T., K. R. C., S. W. K., and R. G. G., unpublished data). Together, these findings are consistent with growing evidence supporting the role of altered connexin distribution in arrhythmogenesis (Kirchoff et al., 1998; Simon et al., 1998; van der Velden et al., 1998).

Recently, minK (or IsK or KCNE1), a small protein that heterodimerizes with KvLQT1 to generate a delayed rectifier $K^+$ current in mammalian cardiac myocytes (Barhanin et al., 1996), has been shown to be a marker of the cardiac conduction system in the murine heart (Kupershmidt et al., 1999). Since the cardiac expression pattern of *HF-1b* is almost superimposable to that of *minK* during heart development, we analyzed *minK* expression via an RNase protection assay using RNA harvested from the intact ventricle of wild-type, heterozygous, and *HF-1b* mutant mice. While the transcript levels of both *KvLQT1* and *Kv1.5* remain relatively unchanged, there was a significant induction of *minK* in the ventricles of *HF-1b* mutant mice when compared to their littermate controls (Figures 6A and 6B).

To establish whether this increased *minK* mRNA level reflected the ectopic expression of minK outside of the conduction system per se in *HF-1b* mutant mice, the cellular distribution of minK was determined by in situ analyses in hearts at two distinct temporal windows, neonatal and adult (Figures 6C–6H). In wild-type neonatal hearts, *minK* expression was highly expressed in the atrioventricular junction and extended posteriorly in an organized pattern reminiscent of the cardiac conduction tissue along both sides of the interventricular septum (Figures 6C and 6E). In *HF-1b* mutant neonatal hearts, *minK* was detected in the atrioventricular junction at levels similar to those in the wild type. However, the organized expression in the ventricular septum seen in wild-type mice was replaced by a dispersed, intense hybridization signal throughout the septum (Figures 6D and 6F), reflecting a developmental defect in conduction system formation in *HF-1b* mutant mice. In the adult heart of wild-type mice, *minK* mRNA was downregulated in the adult heart to background levels (Figure 6G). In contrast, in the mutant adult hearts, downregulation of *minK* only occurred in the ventricular septum (negative results not shown), while the entire transmural myocardium displayed abundant expression of *minK* (compare Figures 6G and 6H), consistent with the earlier persistent, ectopic expression observed in the mutant neonatal hearts.

### *HF-1b*-Deficient Mice Display Increased Action Potential Duration, Heterogeneity, and Dispersion

To gain insight into the cellular defects responsible for the observed alterations in the ECG and the induced rhythm disturbances, electrophysiological studies were performed on enzymatically isolated adult ventricular cells from wild-type *HF-1b* and $-/-$ mutant littermates using patch-clamp techniques (Figure 7). Action potentials, stimulated at a physiological rate (5 Hz) and measured by whole-cell patch-clamp technique, were significantly prolonged as indicated by the time of 50% repolarization ($+/+ = 10.6 \pm 3.0$ ms versus $-/- = 25.3 \pm 7.4$ ms; $p < 0.08$) and of 90% repolarization ($+/+ = 32.5 \pm 8.7$ ms versus $-/- = 86.3 \pm 15.3$ ms; $p < 0.006$) (Figure 7B). Although the action potential duration revealed intrinsic variability, the pooled APD data demonstrated that, on average, mean action potential duration was significantly prolonged in *HF-1b* mutant cells. The larger scatter of action potential duration (APD) observed in the *HF-1b*-deficient mice suggested a greater spatial heterogeneity of APD in ventricular myocytes compared to wild-type mice. To confirm this hypothesis, action potentials were measured in ventricular myocytes isolated from left ventricular (LV) septal cells and from LV epicardial cells near the apex. The perforated patch-clamp technique was used to ensure APD measurements were obtained under more physiological conditions. Consistent with our previous whole-cell recordings (Figure 7B), septal APDs from *HF-1b* mutant mice were significantly prolonged compared to those from littermate control animals, while apical APDs were not significantly different (Table 1). Interestingly, APDs obtained from the septal endocardial cells of *HF-1b* mutant animals were significantly prolonged compared to apical cells, reflecting greater transmural heterogeneity of repolarization in the *HF-1b* mutant mice.

### *HF-1b*-Deficient Mice Display a Decrease in the Density of a Delayed Rectifier $K^+$ Current

Earlier work in normal adult mouse ventricular myocytes has shown that depolarizing voltage-clamp steps activate a number of outward $K^+$ conductances (Zhou et al., 1998; Xu et al., 1999a): qualitatively, these can be described as a $Ca^{+2}$-independent transient outward current and a rapidly activating, slowly inactivating delayed rectifier $K^+$ current. Since action potential duration is regulated at least in part by repolarizing $K^+$ currents, these conductances were measured under voltage-clamp. The superimposed current records in Figure 7C demonstrate that the rapidly activating, slowly inactivating delayed rectifier in myocytes from homozygotes was significantly decreased. In contrast, neither the transient outward $K^+$ current nor the $K^+$ current that regulates resting membrane potential ($I_{K1}$) were changed significantly when control and *HF-1b*-deficient myocytes were compared (Figure 7C). The I–V plots in Figure 7D show that $K^+$ current (measured at the peak and at the end of the 500 ms voltage-clamp steps) was reduced substantially at membrane potentials corresponding to the plateau and repolarization phases of the action potential. Taken together, these results suggest that a selective reduction in the density of the delayed rectifier ($I_{K, slow}$) is largely responsible for the action potential prolongation and dispersion seen in *HF-1b*$^{-/-}$ mutants (Zhou et al., 1998; Xu et al., 1999b).

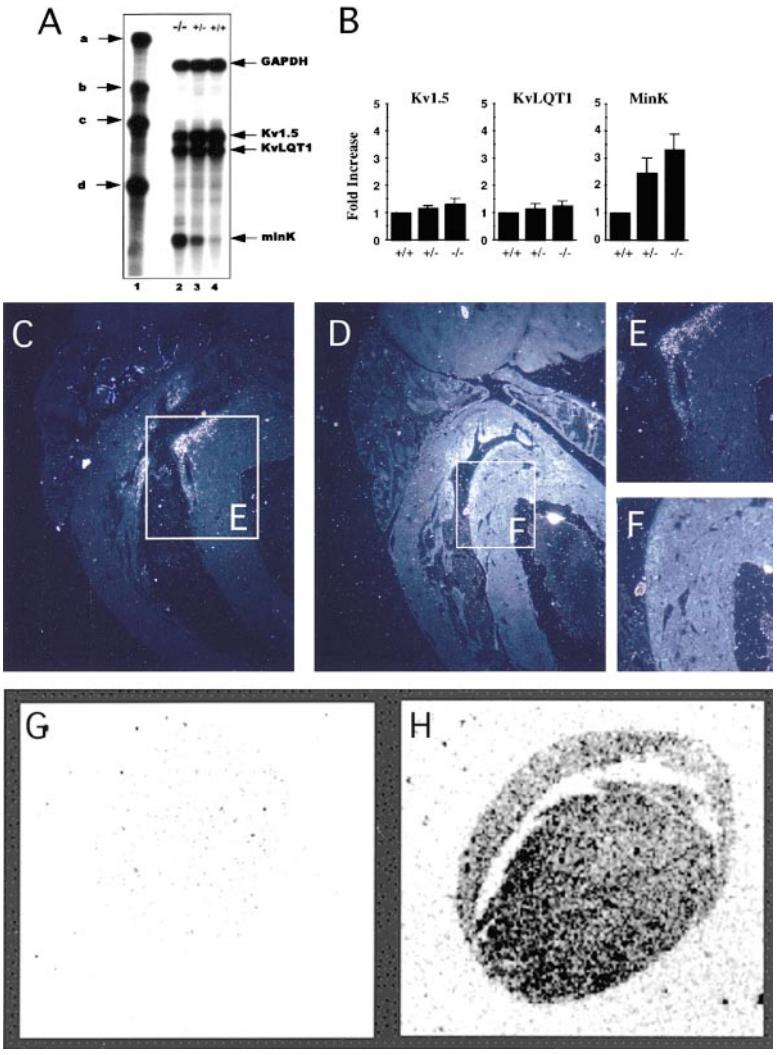


Figure 6. Induction and Mislocalization of *minK* Expression in Ventricles from *HF-1b* Mutant Mice

(A) Representative RNase protection assay of $K^+$ channels *Kv1.5* and *KvLQT1*, and *minK* mRNA levels in *HF-1b*$^{-/-}$ and control mice (+/−, +/+). Note that *minK* is induced while *Kv1.5* and *KvLQT1* remained almost unchanged in *HF-1b*$^{-/-}$ mice. Total RNA (10 μg) from ventricles of *HF-1b*$^{-/-}$ pups (3–4 weeks old) and their littermate controls from independent litters (n = 6) were assayed. Lane 1, unprotected riboprobe sizes of *GAPDH* (a = 403 bp), *Kv1.5* (b = 258 bp), *KvLQT1* (c = 199 bp), and *minK* (d = 135 bp). Lane 2, *HF-1b*$^{-/-}$ (n = 9); Lane 3, *HF-1b*$^{+/-}$ (n = 6); Lane 4, *HF-1b*$^{+/+}$ (n = 7). Protected fragments of *GAPDH* = 316 bp, *Kv1.5* = 181 bp, *KvLQT1* = 170 bp, and *minK* = 106 bp.

(B) Fold increase of *Kv1.5*, *KvLQT1*, and minK mRNAs in *HF-1b* +/+, +/−, and −/− mice. Quantitation of radioactivity was performed and values were normalized with *GAPDH* signal. Fold increase was calculated with value from +/+ mice as a reference of 1.00. *Kv1.5*: +/− = 1.64 ± 0.08; −/− = 1.32 ± 0.2. *KvLQT1*: +/− = 1.14 ± 0.18; −/− = 1.26 ± 0.16. *minK*: +/− = 2.46 ± 0.55; −/− = 3.32 ± 0.58 ($p < 0.01$). Values are mean ± SEM.

(C–H) Comparison of *minK* expression in the wild-type and *HF-1b* mutant hearts at neonatal and adult stage via in situ hybridization. (C) Neonatal wild-type hearts display restricted hybridization signal to the atrioventricular junction and extends as a gradient towards the apex. (D) In *HF-1b* mutant neonatal hearts, *minK* is detected as a diffused signal that includes ventricular septum and ventricular free wall. (E) One hundred times magnification of interventricular septum of wild-type and (F) *HF-1b* mutant neonate. *minK* expression in similar sections from wild-type and mutant adult hearts. (G and H) Signal is reduced to background levels throughout the wild-type heart (G), not detectable by the sensitivity of our method. (H) Strong hybridization signal is detected in epicardial myocytes in *HF-1b* mutant adult hearts.

## Discussion

### *HF-1b* Pathways Play a Critical Role in the Electrophysiological Transition between Ventricular and Conduction System Cell Lineages

Maintenance of normal cardiac rhythm in a mature heart requires the development of specialized pacemaker and conduction system that initiates and propagates the cardiac impulse in a uniform pattern, thus ensuring synchronous contraction and unidirectional blood flow. Conduction system cell lineages include the sinoatrial and atrioventricular nodes that contain pacemaker cells that determine the heart rate, as well as the His-Purkinje system that delivers the impulse to the ventricular myocardium, and is responsible for transmural activation in the left ventricle. Recently, retroviral lineage tracing studies in an avian system have provided compelling evidence that conduction cells are derived from cardiomyogenic precursors in the tubular heart (Cheng et al., 1999). This recruitment process is continuous throughout the early stages of heart development. Successful morphological and functional transition between myogenic and conduction system lineages is critical for establishing the graded changes in action potential duration, pacemaker activity, repolarization, and contractility phenotypes that are distinct features of ventricular, SA nodal, AV nodal, and Purkinje cell lineages. Each of these cells displays a distinct subset of genes that confer the specific electrophysiological phenotype in the central conduction, distal conduction, and ventricular muscle cells. In the ventricular chamber of the mouse, connexin 40 is localized to the myocardial component of the conduction system. In contrast, connexin 43 is predominantly expressed throughout the ventricular myocardium, although coexpression of both Cx40 and Cx43 occurs in some distal Purkinje fiber networks (Gourdie et al., 1993). *minK*, a subunit of one type of heteromeric potassium channel that regulates repolar-

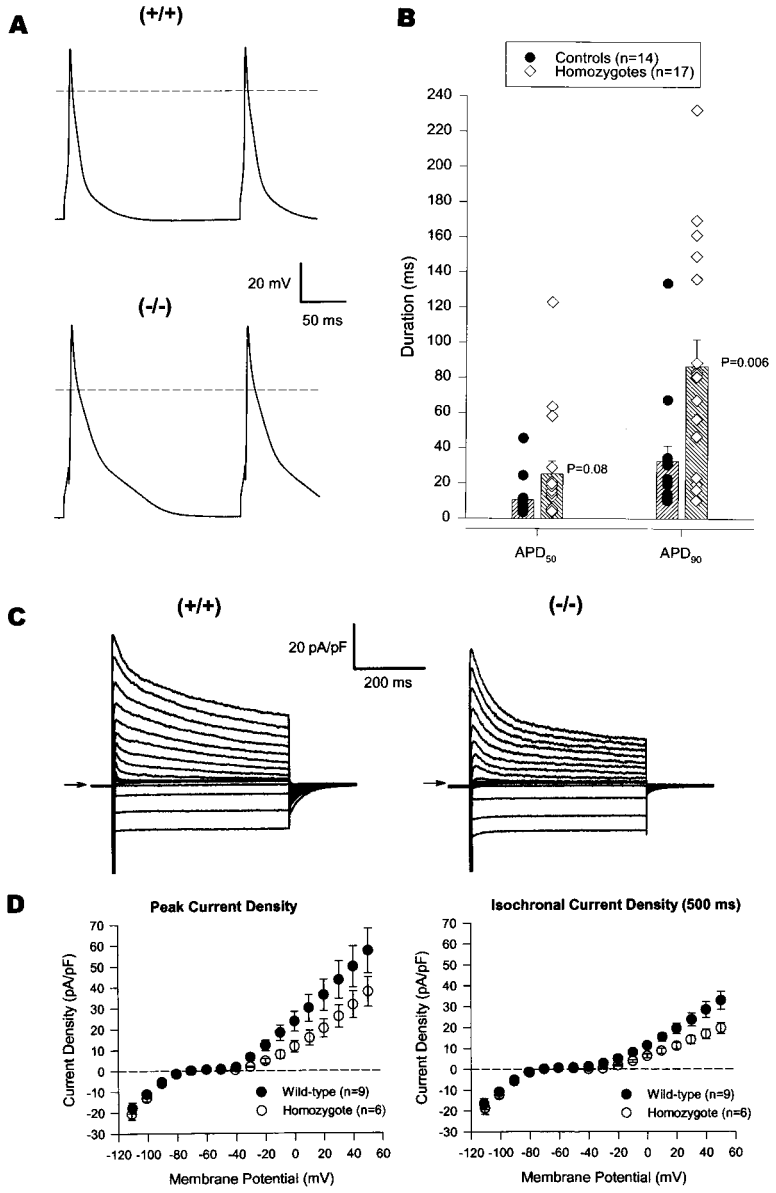


Figure 7. *HF-1b*$^{-/-}$ Mice Have Prolonged and Heterogeneous Action Potential Durations and a Decrease in the Density of a Delayed Rectifier $K^+$ Current

(A) Representative action potentials recorded from ventricular myocytes isolated from control (+/+) and *HF-1b*$^{-/-}$ animals. Stimulation frequency was 5 Hz. Dashed line indicates zero membrane potential. Time and membrane potential calibrations are the same for both action potentials.

(B) Scattergram comparing action potential durations at 50% ($APD_{50}$) and 90% ($APD_{90}$) repolarization from control (n = 14) and *HF-1b*$^{-/-}$ (n = 17) cells. The hatched bars indicate the mean ± SEM for each data group. Note that the difference in mean $APD_{50}$ between controls and *HF-1b*$^{-/-}$ (10.6 ± 3 ms versus 25.3 ± 7.3 ms, respectively) was not statistically significant (p = 0.8, unpaired Student's t test, with Welch's correction). However, the difference in mean $APD_{90}$ (control = 32.5 ± 8.7 ms versus −/− = 86.3 ± 15.3 ms) was statistically significant (p = 0.006).

(C) Representative families of membrane currents from voltage-clamped ventricular myocytes from wild-type (+/+, left panel) and from *HF-1b*$^{-/-}$ (right panel). Currents were activated by 500 ms voltage-clamp steps (from −120 mV to +60 mV, in 10 mV increments). Holding potential was −80 mV. Currents were normalized to cell membrane capacitance in each case: +/+ = 99.4 pF; −/− = 108 pF. Horizontal arrow to the left of each superimposed set of current records indicates the zero current level. Current density and time calibrations are identical for both sets of current records.

(D) Comparison of mean ± SEM current–voltage relationships for ventricular myocytes from +/+ and −/− mice. Peak current density versus membrane potential from 9 +/+ and 6 −/− cells (left panel). Isochronal current density measured at the end of the 500 ms voltage-clamp steps (right panel).

ization of the heart, displays a restricted pattern of expression in the central and distal conduction system, with little expression in ventricular muscle cells per se (Kupershmidt et al., 1999). The precise factors that are responsible for the transition from ventricular to Purkinje fiber cells are unknown. Recently, perivascular derived factors have been implicated by retroviral lineage tracing studies that demonstrated that this transition occurs in close proximity to coronary arterioles.

The present study provides several independent lines of evidence to support a critical role of *HF-1b*/SP4, a member of the SP-1 transcription factor gene family, in the electrophysiological transition between ventricular and conduction system cell lineages. As documented via a knockin of *lacZ* into the endogenous locus, the *HF-1b* gene displays a restricted pattern of expression within the ventricular chamber and is preferentially expressed in conduction system lineages, including the AV node, the atrioventricular ring, branching bundles in the interventricular septum, and the distal His-Purkinje fibers. The timing of onset of *HF-1b* appearance during cardiac development coincides with the process of the recruitment of myogenic precursors into the conduction system. Mice that harbor a complete deficiency in *HF-1b* display a 100% penetrance of severe conduction defects that are evident in the entire conduction system. The expression pattern of conduction system–specific markers are markedly abnormal with a decrease in the number of distal Purkinje fiber cells and an upregulation of a conduction system–specific marker, e.g., minK, in the ventricular chamber. Further evidence of defects in the electrophysiological phenotype of ventricular muscle cells includes a marked increase in action potential heterogeneity (prolonged action potentials in septal endocardial cells but not in apical epicardial cells), a selective decrease of the rapidly activating, delayed rectifier

Table 1. Spatial Dispersion of Action Potential Duration[a]

| | Control | −/− |
|---|---|---|
| Septal Endocardial | 67.2 ± 8.0 (13) | 92.9 ± 6.5 (15)[b,c] |
| Apical Epicardial | 53.4 ± 4.9 (15) | 48.9 ± 12.2 (8) |

[a] APD (ms) measured at 90% repolarization.
[b] $p < 0.009$ control septal versus −/− septal cells.
[c] $p < 0.001$ −/− septal versus −/− apical cells.

$K^+$ current and sudden cardiac death characterized by ventricular arrhythmias. Remarkably, all of the phenotypes in the *HF-1b* mice were restricted to features that control the electrophysiological phenotype of ventricular muscle and conduction system cells, with no effects on cardiac chamber morphogenesis, dilation, hypertrophy, or basal contractile function. Thus, a *HF-1b*-dependent pathway appears to selectively orchestrate the electrophysiological phenotype of ventricular muscle cells, which results in the defective formation of conduction system cell lineages.

*HF-1b* contains an SP-1-like C2H2 zinc finger DNA binding domain and has previously been shown to act as a transcriptional activator in ventricular muscle cells (Zhu et al., 1993). Since transgenic mice that conditionally overexpress *HF-1b* in the ventricular muscle do not display any conduction system defects at the physiological level (data not shown), it is unlikely that *HF-1b* is acting dominantly to promote the conversion of ventricular muscle cells to conduction system lineages. Clearly, other cues are required, and the possibility exists that *HF-1b* may be acting as a positive regulator for the activation of distinct panels of ion channels and connexins in both lineages. The development of mice that harbor lineage-restricted mutations in *HF-1b* with cre-lox technology (Chen et al., 1998; Hirota et al., 1999) should allow a critical examination of the mechanistic pathways and downstream target genes in the *HF-1b* pathway that controls the electrophysiological transition of ventricular to conduction system cells.

### A Genetically Based Model of Cardiac Sudden Death due to Ventricular Arrhythmias in *HF-1b*-Deficient Mice

The development of genetically based mouse models to study the factors responsible for sudden cardiac death due to lethal arrhythmias has proven to be a significant challenge. The mouse model poses several problems arising from (1) its rapid heart rate, (2) a short refractory period, and (3) the small mass of the mouse heart, which has been proposed to confer resistance to ventricular fibrillation (Jalife, 1999). The difficulty is compounded by differences in the ionic currents that underlie the action potential between mouse and larger mammalian species and the technological difficulties of the long-term, continuous, and accurate acquisition of the electrocardiographic monitoring required to capture the sudden death event. Mice that harbor mutant channel genes identical to those found in the human long QT studies do not display a sudden cardiac death phenotype, although arrhythmias can sometimes be detected (Folco et al., 1997; Barry et al., 1998; London et al., 1998). Similarly, a knockout of the *minK* gene, a critical component of the potassium channel that is defective in a subset of long QT patients, does not produce any evidence of arrhythmias or lethality (Charpentier et al., 1998; Drici et al., 1998). To date, there have been no previous reports of genetically based mouse models of authenticated sudden cardiac death. The results of the present study support the concept that the mouse can be engineered to be a valid model of cardiac sudden death, and the technology exists to accurately quantitate complex rhythm disturbances, even in animals at an early age with spontaneous heart rates in excess of 500 beats per minute. The insights gained from the monitoring data suggest that it will indeed be feasible to identify modifiers of this complex electrophysiological phenotype in a manner analogous to what has already been accomplished with regard to contractility and heart failure phenotypes (Chien, 1999; Hirota et al., 1999; Minamisawa et al., 1999). It will become of particular interest to interbreed *HF-1b*$^{-/-}$ mice with strains that harbor modifications in targets that have been proposed to suppress or promote the sudden death phenotype.

### Defects in the Transition between Ventricular and Conduction System Cell Lineages: A New Mechanistic Pathway for Cardiac Sudden Death

Although sudden cardiac death is a major manifestation of heart disease, understanding of the mechanism that leads to its onset is very limited at present. Recently, the discovery of heritable mutations in potassium and sodium channel genes that can confer a risk for sudden death due to their effects on prolonging the QT interval and the action potential duration were reported (Curran et al., 1999; Roden and Spooner, 1999). However, only 20% of family members harboring the disease gene ultimately display the cardiac sudden death phenotype. In addition, sudden cardiac death in its most common form is associated with cardiomyopathy and/or heart failure in the absence of ion channel mutations per se. These considerations strongly suggest that additional pathways to induce sudden death must exist. The discovery of this "second hit" required to produce sudden death would be of importance in understanding the pathways that control normal cardiac rhythm and in identifying new therapeutic targets to intervene in this disease. Currently, cardiac sudden death is largely untreatable via drug-based approaches, and implantable defibrillators are the only currently accepted form of therapy.

The present study provides clear evidence that defects in the pathways that guide and/or maintain the recruitment of ventricular cells into the conduction system lineage may underlie the onset of serious life-threatening ventricular arrrythmias and sudden death. In the absence of *HF-1b*, there is a selective dysregulation of a panel of genes that are involved in the divergent electrophysiological phenotypes of these distinct cell types. This produces a "confused" electrophysiological identity of both ventricular and conduction system lineages characterized by action potential prolongation, dispersion, and heterogeneity, i.e., the anatomic substrate for lethal ventricular arrhythmias. As a result, stochastic events eventually lead to the onset of sudden cardiac death due to lethal ventricular arrhythmias that are classically found in the setting of severe end stage

heart failure. Since the *HF-1b*$^{-/-}$ mice display no evidence of heart failure per se, the *HF-1b* pathway can act as a primary pathway for cardiac sudden death, thereby raising the question as to whether defects in the *HF-1b* pathway may contribute to the increased incidence of sudden death and lethal ventricular arrhythmias seen in the setting of acquired forms of dilated cardiomyopathy and heart failure in humans. This hypothesis should now be testable, and if confirmed, the identification of the downstream and upstream targets in the *HF-1b* pathway via cardiovascular genomic strategies (Chien, 2000) may ultimately lead to the development of more biologically targeted therapeutic strategies for lethal ventricular arrhythmias and sudden cardiac death.

## Experimental Procedures

### Generation of *HF-1b*-Deficient Mice

The targeting construct was made from a 10 kb genomic fragment of *HF-1b* isolated from a 129SVJ mouse genomic library. Out of 120 G418-resistant ES clones, eight were identified as homologous recombinants based on Southern blot hybridization analysis. Two of the eight positive clones were microinjected into J1 129SVJ blastocysts that were subsequently transferred to pseudopregnant females. Chimeric male mice were crossed with Black Swiss breeders.

### Histochemical Analysis

Whole-mount enzyme histochemical detection of the β-galactosidase activity in developing embryos (Ross et al., 1996) and immunohistochemical analysis of connexin 40 (Gourdie et al., 1993) was performed using previously described protocols. All immunohistochemical analyses were analyzed by laser scanning confocal microscopy.

### Electrocardiographical Analyses of *HF-1b*-Deficient Mice

A custom, miniaturized in vivo electrophysiological monitoring system and programmed stimulation protocol were used in these studies. A custom-designed linear electrode array, which consisted of 3 bipolar pairs (interelectrode distance 1 mm), was placed on the anterior–ventricular surface of each heart to deliver stimuli and record electrophysiological data.

### Telemetric Analysis of Electrocardiograms from *HF-1b* Mice

Data were acquired by using an implantable radio frequency transmitter (Data Sciences, St. Paul, MN, TA 10ETA-F20) with subcutaneous leads surgically placed in the conventional lead II position. Precise and stabilized placement of the ECG leads were critical to allow continuous acquisition of the ECG waveforms over a long period of time with relatively low signal-to-noise tracings. Hardware modifications to provide unlimited memory space were necessary to allow continuous, on-line acquisition of electrocardiographic data in the waveform format from multiple instrumented animals.

### Electrophysiological Recordings of Isolated Ventricular Cardiomyocytes

Preparation of adult ventricular myocytes and electrophysiological assessments were performed as previously described (Fiset et al., 1997; Ward and Giles, 1997).

### In Situ Hybridization and RNase Protection Analyses

In situ hybridization with SphI-digested antisense minK probe (EST clone NM008424) was performed as previously described (Ruiz-Lozano et al., 1998). Mouse riboprobes used in RNase protection assays were transcribed from cloned cDNA fragments generated by PCR amplifications with specific oligonucleotide primers: (1) Kv1.5 (AL22218): forward, 5′-gcgggatccATGGAGATCTCCCTGG; reverse, 5′-gcggaattcCCGCATCCTCGTGTGT. (2) KvLQT1 (AU70068): forward, 5′-gcgggatccGAAGCACTTCAACCGG; reverse, 5′-cgcggtaccCCATGACAGACTTTTTAGG. (3) minK (GenBank AX60457): forward, 5′-gcggatccATGAGCCTGCCCAATT; reverse, 5′-cgcggtaccGCTGAGACTTACGAGC.

### Acknowledgments

We thank F. Abdel-Wahab, C. Kondo, B. Poon, J. Anderson, J. Kleint, J. D. Tran, and X. H. Gao for their expert assistance. This work was supported by the National Institutes of Health, the Jean Le Ducq Foundation, and an Endowed Chair of the AHA to K. R. C., an MRC Group Award and the Heart and Stroke Foundation of Alberta Research Chair to W. R. G., and the AHA to S. W. K. and P. R. L.

Received September 18, 1998; revised June 30, 2000.

## References

Abbott, G.W., Sesti, F., Splawski, I., Buck, M.E., Lehmann, M.H., Timothy, K.W., Keating, M.T., and Goldstein, S.A. (1999). MiRP1 forms Ikr potassium channels with HERG and is associated with cardiac arrhythmias. Cell *97*, 175–187.

Angst, B.D., Khan, L.U., Severs, N.J., Whitely, K., Rothery, S., Thompson, R.P., Magee, A.I., and Gourdie, R.G. (1997). Dissociated spatial patterning of gap junctions and cell adhesion junctions during postnatal differentiation of ventricular myocardium. Circ. Res. *80*, 88–94.

Barry, D.M., Xu, H., Schuessler, R.B., and Nerbonne, J.M. (1998). Functional knockout of the transient outward current, long QT syndrome, and cardiac remodeling in mice expressing a dominant-negative Kv4 alpha subunit. Circ. Res. *83*, 560–567.

Barhanin, J., Lesage, F., Guillemare, E., Fink, M., Lazdunski, M., and Romey, G. (1996). KvLQT1 and IsK (minK) protein associate to form the I(Ks) cardiac potassium current. Nature *384*, 78–80.

Charpentier, F., Merot, J., Riochet, D., Le Marec, H., and Escande, D. (1998). Adult KCNE1-knockout mice exhibit a mild cardiac cellular phenotype. Biochem. Biophys. Res. Comm. *251*, 806–810.

Chen, J., Kubalak, S.W., and Chien, K.R. (1998). Ventricular muscle-restricted targeting of the RXRalpha gene reveals a non-cell-autonomous requirement in cardiac chamber morphogenesis. Development *125*, 1943–1949.

Cheng, G., Litchenberg, W.H., Cole, G.J., Mikawa, T., Thompson, R.P., and Gourdie, R.G. (1999). Development of the cardiac conduction system involves recruitment within a multipotent cardiomyogenic lineage. Development *126*, 5041–5049.

Chien, K.R. (1999). Stress pathways and heart failure. Cell *98*, 555–558.

Chien, K.R. (2000). Genomic circuits and the integrative biology of complex cardiac diseases. Nature *406*, in press.

Coral-Vazquez, R., Cohn, R.D., Moore, S.A., Hill, J.A., Weiss, R.M., Davisson, R.L., Straub, V., Barresi, R., Bansal, D., Hrstka, R.F., et al. (1999). Disruption of the sarcoglycan-sarcospan complex in vascular smooth muscle: a novel mechanism for cardiomyopathy and muscular dystrophy. Cell *98*, 465–474.

Curran, M.E., Sanguinetti, M.C., and Keating, M.T. (1999). Molecular basis of inherited cardiac arrhythmias. In Molecular Basis of Cardiovascular Disease, K. Chien, ed. (Cambridge, MA: W.B. Saunders Co.), pp. 302–311.

Delorme, B., Dahl, E., Jarry-Guichard, T., Marics, I., Briand, J.-P., Willecke, K., Gros, D., and Theveniau-Ruissy, M. (1995). Developmental regulation of connexin 40 gene expression in mouse heart correlates with the differentiation of the conduction system. Dev. Dynam. *204*, 358–371.

Drici, M.-D., Arrighi, I., Chouabe, C., Mann, J.R., Lazdunski, M., Romey, G., and Barhanin, J. (1998). Involvement of IsK-associated $K^+$ channel in heart rate control of repolarization in a murine engineered model of Jervell and Lange-Nielsen syndrome. Circ. Res. *83*, 95–102.

Fiset, C., Clark, R.B., Larsen, T.S., and Giles, W.R. (1997). A rapidly activating sustained $K^+$ current modulates repolarization and excitation-contraction coupling in adult mouse ventricle. J. Physiol. *504*, 557–563.

Folco, E., Mathur, R., Mori, Y., Buckett, P., and Koren, G. (1997). A cellular model for long QT syndrome trapping of heteromultimeric

complexes consisting of truncated Kv1.1 potassium channel polypeptides and native Kv1.4 and Kv1.5 channels in the endoplasmic reticulum. J. Biol. Chem. *272*, 26505–26510.

Gourdie, R.G., Severs, N.J., Green, C.R., Rothery, S., Germroth, P., and Thompson, R.P. (1993). The spatial distribution and relative abundance of gap-junctional connexin40 and connexin43 correlate to functional properties of components of the cardiac atrioventricular conduction system. J. Cell Sci. *105*, 985–991.

Gourdie, R.G., Kubalak, S.W., and Mikawa, T. (1999). Conducting the embryonic heart: orchestrating development of cardiac specialized tissues. Trends Cardiovasc. Med. *9*, 17–25.

Hirota, H., Chen, J., Betz, U.A.K., Rajewsky, K., Gu, Y., Ross, J., Jr., Muller, W., and Chien, K.R. (1999). Loss of a gp130 cardiac muscle cell survival pathway is a critical event in the onset of heart failure during biomechanical stress. Cell *97*, 189–198.

Jalife, J. (1999). Spatial and temporal organization in ventricular fibrillation. Trends Cardiovasc. Med. *9*, 119–127.

Kirchoff, S., Nelles, E., Hagendorff, A., Kruger, L., Traub, O., and Willecke, K. (1998). Reduced cardiac conduction velocity and predisposition to arrhythmias in connexin 40-deficient mice. Curr. Biol. *8*, 299–302.

Kubalak, S.W., Doevendans, P.A., Rockman, H.A., Hunter, J.J., Tanaka, N., Ross, J., Jr., and Chien, K.R. (1996). Molecular analysis of cardiac muscle diseases via mouse genetics. In Methods of Molecular Genetics, vol. 8 (Human Molecular Genetics), K.W. Rudolph, ed. (San Diego, CA: Academic Press), pp. 470–487.

Kupershmidt, S., Yang, T., Anderson, M.E., Wessels, A., Niswender, K.D., Magnuson, M.A., and Roden, D.M. (1999). Replacement by homologous recombination of the *minK* genen with *lacZ* reveals restriction of *minK* expression to the mouse cardiac conduction system. Circ. Res. *84*, 146–152.

Litchenberg, W.H., Norman, L.W., Holwell, A.K., Martin, K.L., Hewett, K.W., and Gourdie, R.G. (2000). The rate and anisotropy of impulse propagation in the postnatal terminal crest are correlated with remodeling of Cx43 gap junction pattern. Cardiovasc. Res. *45*, 379–387.

London, B., Jeron, A., Zhou, J., Buckett, P., Han, X., Mitchell, G.F., and Koren, G. (1998). Long QT and ventricular arrhythmias in transgenic mice expressing the N terminus and first transmembrane segment of a voltage-gated potassium channel. Proc. Natl. Acad. Sci. USA *95*, 2926–2931.

Marban, E. (1999). Molecular Basis of Cardiovascular Disease (companion text to E. Braunwald's Heart Disease), K.R. Chien, ed., J. Breslow, J. Leiden, R. Rosenberg, and C.E. Seidman, section eds. (Cambridge, MA: W.B. Saunders Co.).

Minamisawa, S., Hoshijima, M., Chu, G., Ward, C.A., Frank, K., Gu, Y., Martone, M.E., Wang, Y., Ross, J., Jr., Kranias, E.G., et al. (1999). Chronic phospholamban-sarcoplasmic reticulum calcium ATPase interaction is the critical calcium cycling defect in dilated cardiomyopathy. Cell *99*, 313–322.

Roden, D.M., and Spooner, P.M. (1999). Inherited long QT syndromes: a paradigm for understanding arrhythmogenesis. J. Cardiovasc. Electrophysiol. *10*, 1664–1683.

Ross, R.S., Navansakasattusas, S., Harvey, R.P., and Chien, K.R. (1996). An HF-1a/*HF-1b*/MEF-2 combinatorial element confers cardiac ventricular specificity and establishes an anterior-posterior gradient of expression. Development *122*, 1799–1809.

Ruiz-Lozano, P., Smith, S.M., Perkins, G., Kubalak, S.W., Boss, G.R., Sucov, H.M., Evans, R.M., and Chien, K.R. (1998). Energy deprivation and a deficiency in downstream metabolic target genes during the onset of embryonic heart failure in RXR$\alpha$ $-/-$ embryos. Development *125*, 533–544.

Simon, A.M., Goodenough, D.A., and Paul, D.L. (1998). Mice lacking connexin 40 have cardiac conduction abnormalities characteristic of atrioventricular block and bundle branch block. Curr. Biol. *8*, 295–298.

Supp, D.M., Witte, D.P., Branford, W.W., Smith, E.P., and Potter, S.S. (1996). Sp4, a member of the Sp1-family of zinc finger transcriptional factors, is required for normal murine growth, viability, and male fertility. Dev. Biol. *176*, 284–299.

van der Velden, H.M., van Kempen, M.J., Wijffels, M.C., van Zijverden, M., Groenewegen, W.A., Allessie, M.A., and Jongsma, H.J. (1998). Altered pattern of connexin40 distribution in persistent atrial fibrillation in the goat. J. Cardiovas. Electrophysiol. *9*, 596–607.

Ward, C.A., and Giles, W.R. (1997). Ionic mechanism of the effects of hydrogen peroxide in rat ventricular myocytes. J. Physiol. (Lond.) *500*, 631–642.

Xu, H., Barry, D.M., Li, H., Brunet, S., Guo, W., and Nerbonne, J.M. (1999a). Attenuation of the slow component of delayed rectification, action potential prolongation and triggered activity in mice expressing a dominant-negative Kv2 $\alpha$subunit. Circ. Res. *85*, 623–633.

Xu, H., Guo, W., and Nerbonne, J.M. (1999b). Four kinetically distinct depolarization-activated $K^+$ currents in adult mouse ventricular myocytes. J. Gen. Physiol. *113*, 661–677.

Zipes, D.P., and Wellens, H.J.J. (1998). Sudden cardiac death. Circulation *98*, 2334–2351.

Zhou, J., Jeron, A., London, B., Han, X., and Koren, G. (1998). Characterization of a slowly inactivating outward current in adult mouse ventricular myocytes. Circ. Res. *83*, 806–814.

Zhu, H., Nguyên, V.T.B., Brown, A., Pourhosseini, A., Garcia, A.V., van Bilsen, M., and Chien, K.R. (1993). A novel, tissue restricted zinc finger protein (HF1-b) binds to the cardiac regulatory element (HF1-b/MEF-2) in the rat myosin light chain-2 gene. Mol. Cell. Biol. *13*, 4432–4444.